Biodegradation (2007) 18:453–464
DOI 10.1007/s10532-006-9078-2

ORIGINAL PAPER

A mathematical model for the kinetics of *Methanobacterium bryantii* M.o.H. considering hydrogen thresholds

Fatih Karadagli · Bruce E. Rittmann

Received: 16 June 2006 / Accepted: 8 August 2006 / Published online: 10 November 2006

Abstract We develop a kinetic model that builds on the foundation of classic Monod kinetics, but incorporates new phenomena such as substrate thresholds and survival mode observed in experiments with the H_2-oxidizing methanogen *Methanobacterium bryantii* M.o.H. We apply our model to the experimental data presented in our companion paper on H_2 thresholds. The model accurately describes H_2 consumption, CH_4 generation, biomass growth, substrate thresholds, and survival state during batch experiments. Methane formation stops when its Gibbs free energy is equal zero, although this does not interrupt H_2 oxidation. The thermodynamic threshold for H_2 oxidation occurs when the free energy for oxidizing H_2 and transferring electrons to biomass is no longer negative, at ~0.4 nM. This threshold is not controlled by the Gibbs free energy equation of methanogenesis from H_2 + HCO_3^- as we show in our companion paper. Beyond this threshold, the microorganisms shift to a low-maintenance metabolism called ‘‘the survival state’’ in response to extended H_2 starvation; adding the starvation response as another new feature of the kinetic model. A kinetic threshold (or S_{min}), a natural feature of the Monod kinetics, is also captured by the model at H_2 concentration of around ~2,400 nM. S_{min} is the minimum substrate concentration to maintain steady-state biomass concentration. Our model will be useful for interpreting threshold results and designing new studies to understand thresholds and their ecological implications.

Keywords Kinetic model · Hydrogen thresholds · Survival · Gibbs free energy · Methanogens

F. Karadagli · B. E. Rittmann
Department of Civil and Environmental Engineering, Northwestern University, 2145 Sheridan Road, Evanston, IL 60208-3109, USA

F. Karadagli (✉)
Department of Environmental Engineering, School of Engineering, Sakarya University, Sakarya 54187, Turkey
e-mail: fkaradagli@sakarya.edu.tr

Present Address:
B. E. Rittmann
Center for Environmental Biotechnology, Biodesign Institute at Arizona State University, 1001 South McAllister Avenue, P.O. Box 875701, Tempe, AZ 85287-5701, USA

Introduction

Respiring microorganisms consume H_2 until a certain minimum level that is called the H_2 threshold, which is a minimum concentration below which consumption of H_2 by the particular microorganism stops (Lovley 1985; Widdel 1988;

Conrad 1996). Several studies proposed that H_2 thresholds are controlled by thermodynamics, specifically having the Gibbs free energy (ΔG) equal zero (Cord-Ruwisch et al. 1988; Lovley and Goodwin 1988; Chapelle et al. 1996; Hoehler et al. 1998; Yang and McCarty 1998). Solving the Gibbs equation for H_2 at $\Delta G = 0$ gives the strict-thermodynamic H_2 threshold, which can be computed if standard free energies, temperature, and concentrations of all reactants and products are known for the reaction.

In our companion article (Karadagli and Rittmann 2006, companion), we investigated H_2 thresholds systematically using methanogenesis and *Methanobacterium bryantii* M.o.H., which uses H_2 as its only electron donor. We computed the strict thermodynamic H_2 threshold from the Gibbs equation for each batch experiment and compared these values to the experimental observations. Our comparison showed that the H_2 threshold for *M. bryantii* was not controlled by the Gibbs free energy relationship for methanogenesis with H_2, but often was lower than the values computed with Gibbs equation. We found a reproducible a constant H_2 threshold of ~0.4 nM (with a range of 0.2–1 nM) for batch experiments in which the strict-thermodynamic thresholds ranged from 0.2 to 4 nM, depending on the activity of methane.

On the one hand, the strict thermodynamic and actual thresholds may differ, because the Gibbs equation is applicable only for reversible reactions that can reach a true thermodynamic equilibrium. Because the last step of methane production is a one-way (irreversible) reaction (Thauer 1998), an equilibrium-based H_2 threshold should not be relevant for methane production from $H_2 + HCO_3^-$. In parallel to methanogenesis, the last steps of other dissimilatory reactions also are irreversible (Hollocher 1982; Legall and Fauque 1988; Stouthamer 1988; Nicholls and Ferguson 2002); therefore, computation of H_2 thresholds by using Gibbs free energy equation is not feasible in a general sense.

On the other hand, H_2 oxidation by *M. bryantii* and by other dissimilatory anaerobic microorganisms is a reversible reaction (Karadagli and Rittmann 2006, companion; Valentine et al. 2000); thus, a reproducible, equilibrium-based H_2 threshold is possible if the ultimate sink for the electrons receives the electrons in a reversible reaction. Based on the consistency of the observed H_2 threshold and that H_2 was generated by endogenous oxidation of biomass, we (Karadagli and Rittmann 2006, companion) proposed that this reversible reaction is one in which the reduced product is a solid biomass component. Electrons from H_2 oxidation must be transferred to cell's solid components when methanogenesis becomes thermodynamically unfavorable, or the ΔG for methanogenesis is greater than or equal to zero. However, H_2 oxidation continues until $\Delta G = 0$ for the $H_2 \rightarrow$ biomass reaction, which is when the ultimate thermodynamic H_2 threshold is observed.

In parallel to the thermodynamic threshold, we consider a series of physiological changes that occur as the cells reach the threshold and take actions to protect themselves against starvation (Reeve et al. 1984a; Kjelleberg et al. 1987; Siegele and Kolter 1992). When external electron donor is no longer available, some cells execute a program that adjusts their metabolism to survive for the long term. In this program, they reduce cell size by condensing cytoplasm, degrade RNA and other proteins, synthesize new resistant proteins, change cell wall structure toward a hydrophobic composition, and condense DNA. Cells reduce their overall energy demand through these activities so that, during starvation, they can survive by consuming their internal energy sources, such as biomass in general and reserve compounds, e.g., glycogen.

Describing the thermodynamic threshold and the starvation response is new for modeling microbial systems, and we incorporate these two phenomena into a kinetic model that maintains the usual features, which remain in effect when the H_2 concentration is higher than the thermodynamic threshold: H_2 oxidation, methanogenesis, and biomass synthesis and decay. We use *M. bryantii* M.o.H. as our model microorganism consuming H_2 as the sole electron donor and generating methane as the normal end product of respiration. We evaluate the model outputs against the experimental data presented in our companion paper, in which the concentrations of *M. bryantii*, H_2, and CH_4 were measured in batch experiments.

Mathematical model

The model assumes equilibrium between gas and liquid phases for H_2 and CH_4. The total mass of a gaseous compound in a batch system is

$$M_T = \left(\frac{C_L}{R \times T \times K_H}\right) \times V_G + C_L \times V_L \qquad (1)$$

where M_T is the total mass of a gaseous compound in moles, C is the liquid-phase concentration in mol/L, R is the ideal gas constant (0.082 L-atm/mol K), T is the temperature in Kelvin, K_H is the Henry's law constant in mol/L-atm, V is the volume in liters, and G and L identify the gas and liquid phases, respectively. We calculated K_H values for our experimental temperature of 37°C using the van't Hoff equation (Stumm and Morgan 1996): 7.4×10^{-4} mol H_2/L-atm and 1.04×10^{-3} mol CH_4/L-atm.

The change in total mass of hydrogen is only via microbial consumption, which occurs in the liquid phase; therefore,

$$\begin{aligned}\frac{dM_{T,H_2}}{dt} &= \left(\frac{d[H_2]_L}{dt}\right) \times \left(\frac{V_G}{R \times T \times K_H} + V_L\right)\\ &= \left[-q_{max} \times \left(\frac{[H_2]_L}{K_{s,H_2} + [H_2]_L}\right) \times X_a\right] \times V_L \qquad (2)\end{aligned}$$

where [...] denotes concentration in mol/L. The left term on the right side of Eq. 2 is the Monod term for substrate consumption, in which q_{max} is the maximum specific substrate consumption rate (mol H_2/g cells-day), K_{s,H_2} is the half-maximum-rate concentration (mol H_2/L), and X_a is the active biomass concentration (g cells/L).

The change in microbial biomass due to consumption of hydrogen is

$$\begin{aligned}\frac{dX_a}{dt} &= \left[\mu_{max} \times \left(\frac{[H_2]_L}{K_{s,H_2} + [H_2]_L}\right) - b\right] \times X_a\\ &= \left[Y \times q_{max} \times \left(\frac{[H_2]_L}{K_{s,H_2} + [H_2]_L}\right) - b\right] \times X_a \qquad (3)\end{aligned}$$

where μ_{max} is the maximum specific growth rate of the biomass (1/day), b is the endogenous-decay coefficient (1/day), Y is the true yield or the mass of cells synthesized per unit mass of substrate consumed (g cells/mol H_2), and all other terms are as explained before. Y is proportional to the fraction of electrons that the cells must use for synthesis (Namkung and Rittmann 1987; Rittmann and McCarty 2001), $f_s°$, through a unit conversion, which is, for H_2 as the donor,

$$\begin{aligned}f_s^\circ &= (Y)(\text{mol cells}/\text{mol } H_2) \times (1 \text{ mol } H_2/2\text{e eq})\\ f_s^\circ &= (0.325 \text{ g cells}/\text{mol } H_2)*) \times (1 \text{ mol } H_2/2\text{e}^- \text{ eq})*)\\ &\quad \times (20\text{e}^- \text{ eq cells}/\text{mol cells})\\ &\quad \times (1 \text{ mol cells}/113 \text{ g cells}_{(C5H7O2N)})\\ &= 0.029\text{e}^- \text{ cells}/\text{e } H_2.\end{aligned}$$

The mass balance equation for methane, the end product of normal methanogenic metabolism, is

$$\begin{aligned}\frac{dM_{T,CH_4}}{dt} &= \left(\frac{d[CH_4]_L}{dt}\right) \times \left(\frac{V_G}{R \times T \times K_H \times V_L} + 1\right)\\ &= \left[0.25\left(\frac{d[H_2]_L}{dt}\right)(1 - f_s^\circ)\right.\\ &\quad + bX_a\left(1.42\frac{\text{mg COD}}{\text{mg } C_5H_7O_2N}\right)\\ &\quad \left.\times \left(0.25\frac{\text{mg } CH_4}{\text{mg COD}}\right)\left(\frac{1 \text{ mol } CH_4}{16000 \text{ mg}}\right)\right] \qquad (4)\end{aligned}$$

Equation 4 includes methane production due to consumption of hydrogen and endogenous respiration. The first term on the right side of Eq. 4 is the formation of CH_4 based on the total oxidation of H_2 the electron equivalents transferred to newly synthesized biomass ($f_s°$). In this term, 0.25 is the stoichiometric molar ratio of produced CH_4 per mole of oxidized H_2. Endogenous respiration of biomass ($C_5H_7O_2N$) also generates CH_4 in proportion to the electron equivalents removed by oxidation of a mole of biomass, the second term on the right side.

In addition to H_2, biomass, and methane concentrations, the model computes the net free energy for methanogenesis from the Gibbs free energy equation. We explained in our companion paper how we computed activities of reactants and products in our medium (Karadagli and Rittmann 2006, companion). The reaction of methane production from H_2, its Gibbs free energy, and the strict-thermodynamic threshold equation of methanogenesis are

$$1/4HCO_3^- + H_{2(aq)} + 1/4H^+ \rightarrow 1/4CH_{4(aq)} + 3/4H2O_{(l)}$$

$$\Delta G = \Delta G^\circ + R \times T \times \ln \frac{\{CH_4\}_{(aq)}^{0.25} \times \{H_2O\}^{0.75}}{\{HCO_3^-\}^{0.25} \times \{H^+\}^{0.25} \times \{H_2\}_{(aq)}} \quad (5)$$

$$\{H_2\}_{threshold} = \frac{\{CH_4\}_{(aq)}^{0.25} \times \{H_2O\}^{0.75}}{\{HCO_3^-\}^{0.25} \times \{H^+\}^{0.25} \times e^{(-(\Delta G^\circ)/R \times T)}} \quad (6)$$

The standard free energy of methane production at 37°C is $\Delta G^\circ = -59.05$ kJ/mol H_2.

In Eq. 6, activity of water is 1 by definition, pH is fixed in our medium (7.2), bicarbonate activity is much higher than activities of other compounds so that bicarbonate activity is constant (0.03) and thus, the only activity that changes the H_2 threshold is the final methane activity. According to this equation, the H_2 threshold increases along with final methane activity with a range of 0.2–4.9 nM for all experiments in this study. In contrast, we observed that H_2 thresholds remained constant for all experiments and were not affected by the final methane activities (Karadagli and Rittmann 2006, companion). Therefore, we presented an alternate reaction for transfer of electrons from H_2 to solid biomass components; activity of the solid product is always 1, since it is solid, and thus, it does not affect the computed H_2 threshold values. Here we show this reaction, its ΔG, and the threshold equation

$$H_{2(aq)} + 1/2HCO_3^- + 1/2H^+ \rightarrow 1/2CH_2O_{(s)} + H_2O \quad (7)$$

$$\Delta G = \Delta G^\circ + R \times T \times \ln \frac{\{CH_2O_{(s)}\}^{1/2} \times \{H_2O\}}{\{H_{2(aq)}\} \times \{HCO_3^-\}^{1/2} \times \{H^+\}^{1/2}} \quad (8)$$

$$\{H_2\}_{threshold} = \frac{\{CH_2O\}_{(s)}^{0.5} \times \{H_2O\}}{\{HCO_3^-\}^{0.5} \times \{H^+\}^{0.5} \times e^{(-(\Delta G^\circ)/R \times T)}} \quad (9)$$

where $CH_2O_{(s)}$ represents the solid biomass components that accept electrons from H_2 and become reduced. All other parameters are same as before.

In independent experiments (Karadagli and Rittmann 2005), we determined the Monod parameter values for *M. bryantii* M.o.H. Their values are: $\mu_{max} = 0.77$/day; $q_{max} = 2.36$ mol $[H_2]$/g cells/day; $K_s = 18$ µM; $Y = 0.325$ g cells/mol H_2; and $b = 0.09$/day. The minimum H_2 concentration able to support a positive growth rate, $S_{min} = b/(Y \times q_{max} - b)$, is *c*. 2400 nM (Karadagli and Rittmann 2005).

To incorporate the new threshold concept in the model, we stop methane production from H_2 oxidation when ΔG for methanogenesis is zero. This effect is implemented by removing the $(d[H_2]/dt)$ term from the right side of Eq. 4 when ΔG in Eq. 5 is equal to or greater than zero. However, methane production from biomass decay continues (second term on the right of Eq. 4), because electrons from oxidation of biomass can still be transferred to CH_4 (Karadagli and Rittmann 2006, companion). In addition, H_2 oxidation can continue, with the electrons transferred to a solid cell material.

Based on reproducible experimental results (Karadagli and Rittmann 2006, companion), we establish a strict-thermodynamic threshold for H_2 oxidation at 0.4 nM H_2. When the new strict thermodynamic threshold is reached, the model stops H_2 consumption and biomass growth by making $q_{max} = 0$ in Eqs. 2 and 3.

Because the cells cannot gain any energy from H_2 oxidation when $H_2 \leq 0.4$ nM, we then begin the process by which the microorganisms switch into a starvation mode by reducing most metabolic activities, degrading many proteins and RNA, condensing their DNA, and synthesizing new resistant proteins for long-term starvation (Reeve et al. 1984b; Kjelleberg et al. 1987; Siegele and Kolter 1992). To represent starvation mode in the model, we drop the decay rate tenfold, from 0.09 to 0.009/day, 2 days after the H_2 concentration reaches the strict-thermodynamic threshold (0.4 nM). The 2-day transition period is based on the biomass data from the experiments (Karadagli and Rittmann 2006, companion), which showed that the cells had a significantly slowed decay rate by about 2 days after the H_2 threshold reached ~0.4 nM.

We simulated the growth of *M. bryantii* M.o.H. in a batch system by solving the model equations numerically using Microsoft Excel or Matlab (Mathworks Inc., Natick, MA, USA) computer programs. The experimental batch system is described in detail in our companion paper; however, briefly, it is an anaerobic tube with a total volume of 28 mL that is divided into 5 mL liquid medium, 1 mL inoculum, and 22 mL gas phases. We enter the kinetic parameters and the initial values of biomass, H_2, and CH_4 into the equations, and we then compute the outcome with a time interval (Δt) of 0.003 days.

Results and discussion

We compared our model predictions to the experimental results for all experiments in Karadagli and Rittmann (2006, companion). Besides concentrations of biomass, H_2, and CH_4, we computed the net free energies for methanogenesis (Eq. 5) and for the new solid-phase reaction (Eq. 8). All experiments were represented well by the model, and we present comparisons for a set of experiments that illustrate the range of responses. Table 1 summarizes the key information for the experiments presented here. One significant feature is the range of initial biomass concentrations (0.01–0.3 as optical density, OD, or 4.4–73 mg/L as cell-dry weight), which makes it possible to evaluate well how the model represents the lag and exponential-growth phases. A second significant feature is that the final CH_4 concentrations cover a fivefold range. The final CH_4 concentration determines the thermodynamic threshold for methanogenesis, and these ranged from 0.2 to 4.9 nM for the experiments in Table 1. However, the new thermodynamic threshold based on the solid biomass material does not change.

The results in Figs. 1, 2, 3, and 4 show that the new model captures all the key trends in H_2, CH_4, biomass, and the free energy data of the experiments in Table 1. The different figures highlight different aspects of the model. Although the time period for consumption of hydrogen is similar for all three figures (2–4 days), the stability period of the H_2 threshold ranges from 5 to 25 days. Consequently, the time scales for Figs. 1 and 2 are logarithmic for the longer stability periods in order to show the key features of the model and the experimental results, e.g., lag phase, S_{min}, and survival mode.

Figure 1 indicates an extended lag phase of 18 h due to low initial biomass concentration, which distinguishes Fig. 1 from the two figures that follow. Correspondingly, H_2 consumption and CH_4 production are slow during this phase. H_2 is consumed rapidly between days 1 and 2, as cells enter into the logarithmic growth phase, and CH_4 is generated in stoichiometric amounts. Around day 3, the biomass growth rate goes from positive to negative; the H_2 concentration is around 2,400 nM, which corresponds to the kinetically based S_{min} value (Karadagli and Rittmann 2005). That the model captures the lag, logarithmic-growth, and S_{min} phases confirms that the traditional features of the model and the Monod-parameter values are accurate.

Methane is produced significantly for the first 2–3 days of the experiment, when the rate of H_2 oxidation is high and ΔG for methanogenesis is negative. At 3.4 days, ΔG of methane formation from $H_2 + HCO_3^-$ becomes zero, and therefore, methane production stops. Methane production

Table 1 Summary of key experimental conditions simulated by the model

Initial OD_{600}	Initial $[H_2]_{liq}$ (nM)	Initial $[CH_4]_{liq}$ (nM)	Final $[CH_4]_{liq}$ (nM)	Methanogenesis H_2-threshold (nM)	Solid-biomass H_2-threshold (nM)	Figure No.
0.01	213,000	2,000	74,000	3.9	0.4	1
0.3	356,000	255,000	390,000	4.7	0.4	2
0.045	431,000	301,000	440,000	4.9	0.4	3
0.007	55	5	43	0.2	0.4	4

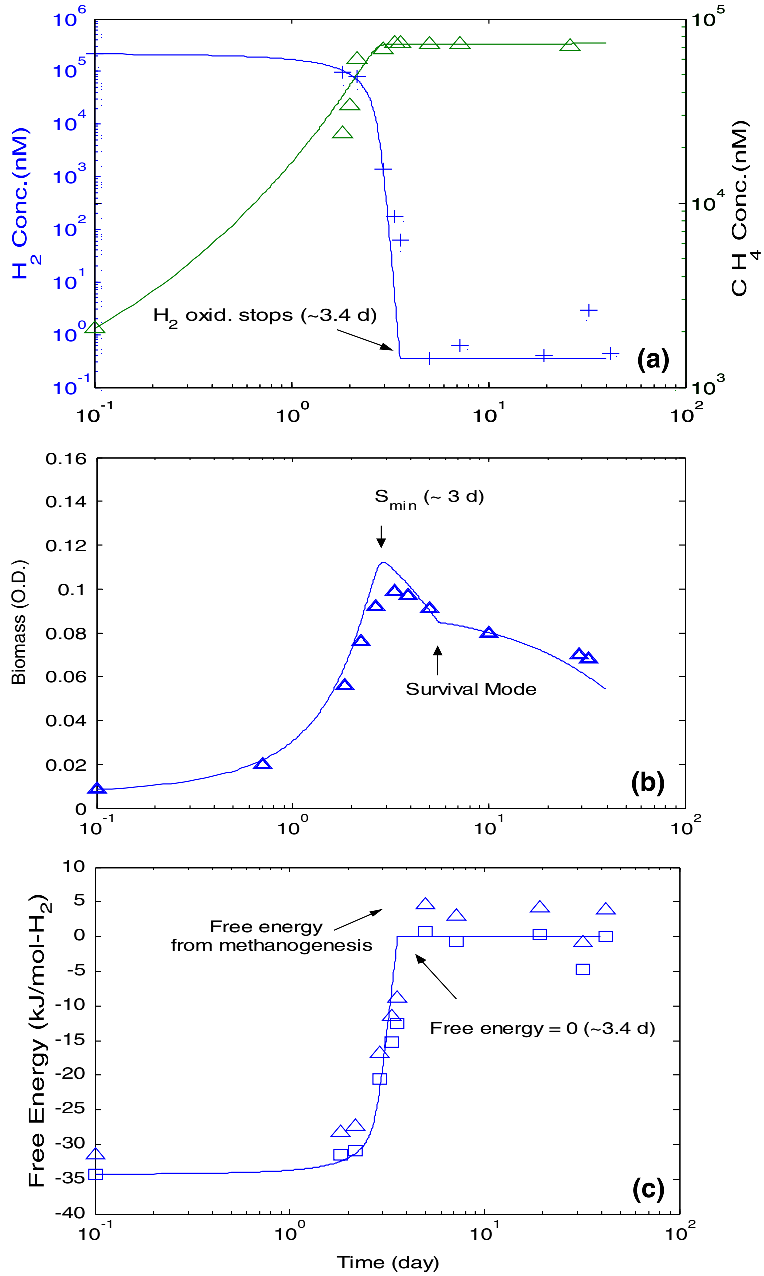

Fig. 1 Experimental results (*symbols*) and model simulations (*lines*) for H_2 threshold experiments with *Methanobacterium bryantii* M.o.H when the initial H_2 concentration was 213,000 nM. **(a)** H_2 (*plus*) and CH_4 (*triangles*), **(b)** biomass concentration as O.D. **(c)** available free energy from methanogenesis (*triangles*) and from biomass reaction (*squares*)

due to endogenous decay continues, but the production rate is small compared to the methane concentration.

The new strict-thermodynamic threshold occurs around 4 days, when H_2 consumption stops at a concentration of 0.4 nM and ΔG for the solid-biomass acceptor reaches zero (Fig. 1a, c). For comparison, the available free energy from methanogenesis with H_2 (Fig. 1c) is positive (+5 kJ/mol H_2) when the strict thermodynamic threshold is observed at ~0.4 nM, which is well below the computed threshold for H_2-to-methane reaction that is 3.9 nM for Fig. 1.

A decrease in the biomass-decay rate is also observed starting on day 6, 2 days after H_2 oxidation stopped around day 4, indicating that cells enter into the survival mode. During the next 30 days, the survival stage is simulated well by the

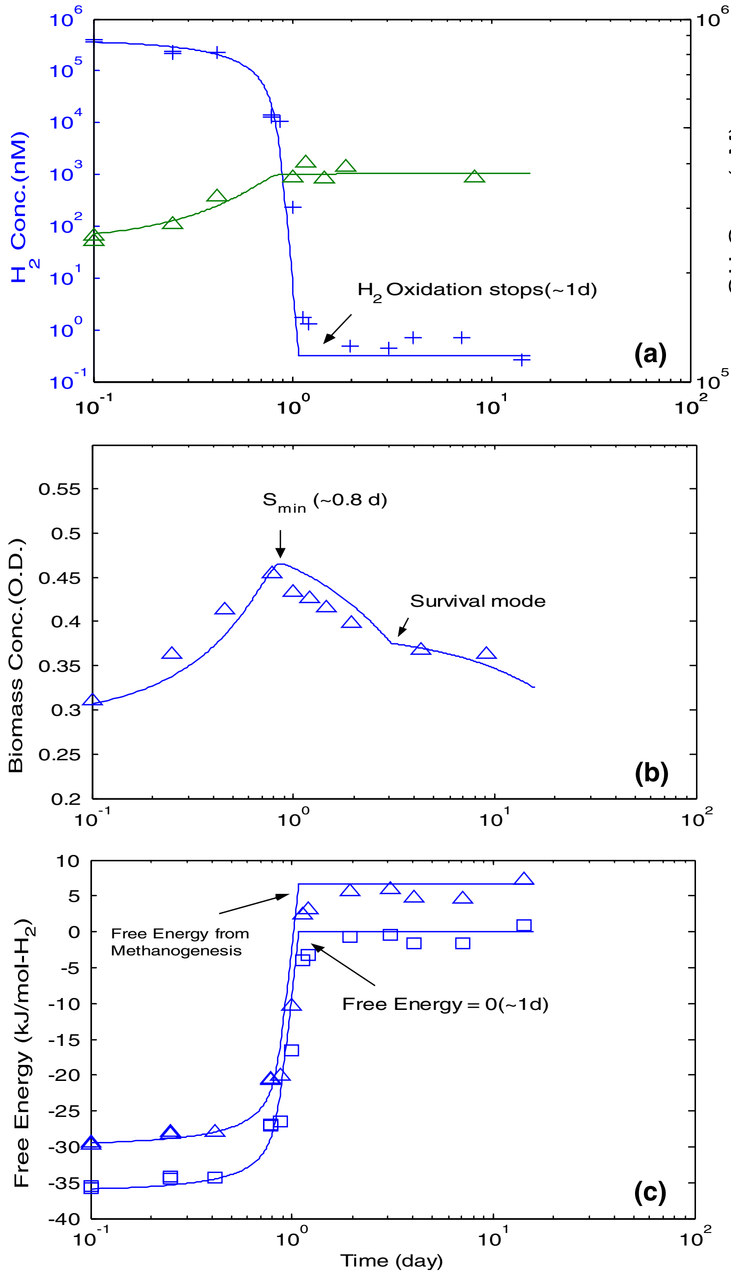

Fig. 2 Experimental results (*symbols*) and model simulations (*lines*) for H_2 threshold experiments with *Methanobacterium bryantii* M.o.H when final CH_4 concentration was 390,000 nM. **(a)** H_2 (*plus*) and CH_4 (*triangles*), **(b)** biomass concentration as O.D., **(c)** available free energy from methanogenesis (*triangles*), and from biomass reaction (*squares*)

model with an endogenous decay constant ten times lower than the normal value.

Figure 2 shows that H_2 consumption, CH_4 generation, and biomass growth started immediately for an experiment in which the initial biomass concentration is relatively large (0.3 O.D.) and CH_4 was added initially to accentuate the differences between the thermodynamic thresholds for methanogenesis and the solid-biomass acceptor. The large initial biomass concentration eliminates the lag phase and compresses the experimental time so that H_2 consumption is complete by 1 day. The model explains that methanogenesis stops when its $\Delta G = 0$, or when H_2 concentration is 4.7 nM, but H_2 oxidation continues to the new threshold of 0.4 nM. Figure 2a clearly shows that H_2 oxidation continues well below 4.7 nM, stopping at the new

Fig. 3 Experimental results (*symbols*) and model simulations (*lines*) for H_2 threshold experiments with *Methanobacterium bryantii* M.o.H when final CH_4 concentration was 440,000 nM. **(a)** H_2 (*plus*) and CH_4 (*triangles*), **(b)** biomass concentration as O.D., **(c)** available free energy from methanogenesis (*triangles*), and from biomass reaction (*squares*)

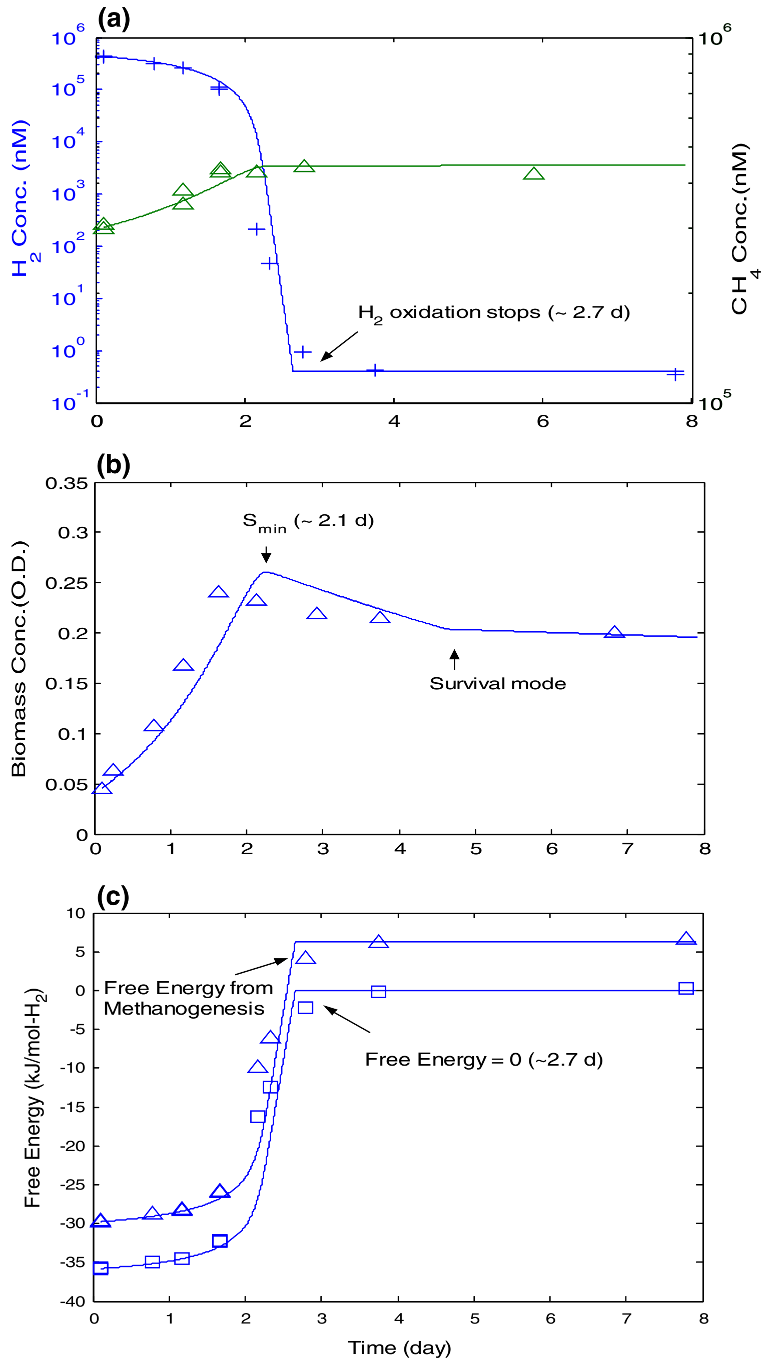

strict-thermodynamic threshold of ~0.4 nM at 1.1 days, while CH_4 generation almost stops at 1 day, slightly before H_2 oxidation stops at the new strict-thermodynamic threshold of 0.4 nM (Fig. 2a).

Despite the short duration of the experiment, S_{min} (2,400 nM) occurs at around 20 h. The cells enter into the survival state (slower decay rate) around 3 days, which is supported by the good match between experimental results and the model predictions out to day 12.

Figure 3 shows that the model simulations and experimental data match well for H_2 consumption, CH_4 generation, and biomass for an exper-

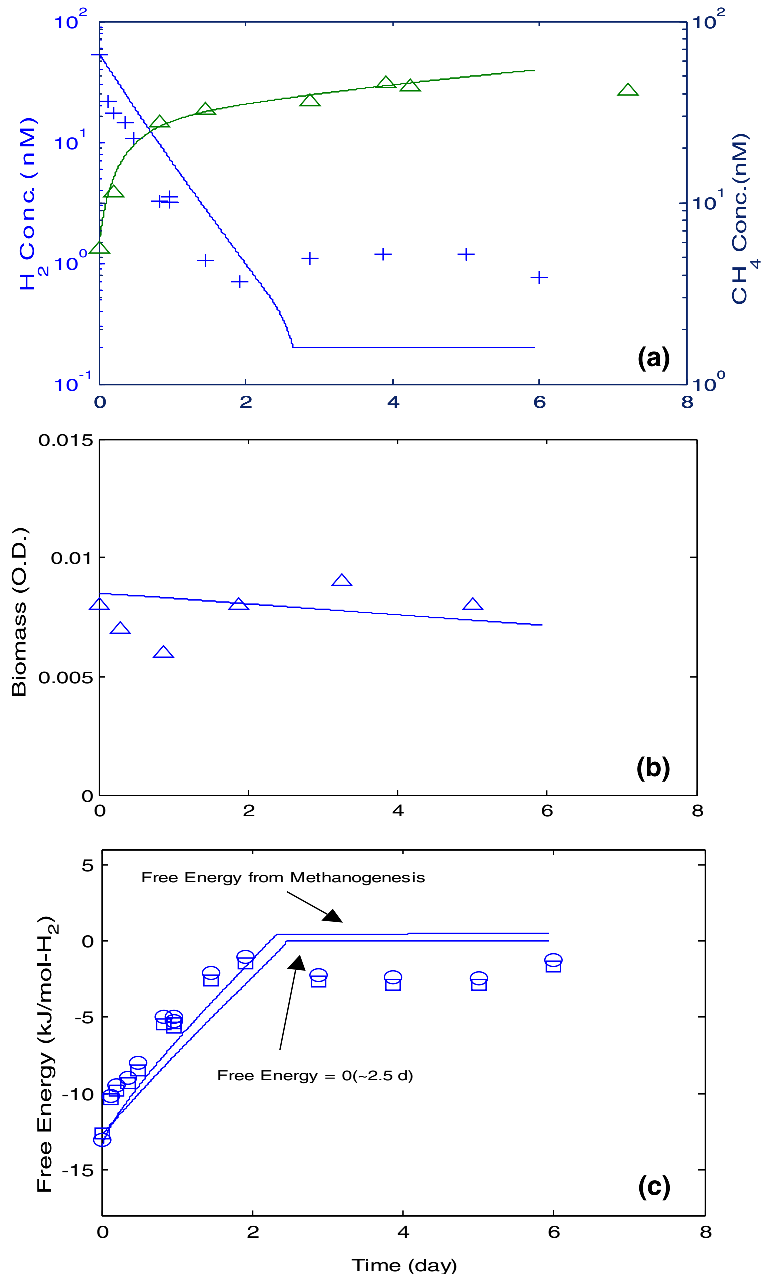

Fig. 4 Experimental results (*symbols*) and model simulations (*lines*) for H_2 threshold experiments with *Methanobacterium bryantii* M.o.H when final CH_4 concentration was 43 nM. **(a)** H_2 (*plus*) and CH_4 (*triangles*), **(b)** biomass, **(c)** available free energy from methanogenesis (*circles*), and from biomass reaction (*squares*)

iment that had a high-thermodynamic threshold for methanogenesis (4.9 nM), but less initial biomass than in the previous experiment. Figure 3a shows that methane generation stops at well before H_2 oxidation, around 2.4 days. Methane concentration plateaus at 440,000 nM when H_2 concentration is around 5–50 nM. Figure 3b shows that S_{min} occurs around 1.9–2.2 days, when experimentally measured H_2 was 6,000–1,000 nM, spanning the computed value of 2,400 nM. The cells enter into survival stage beyond 4 days, as supported by the slowed decay rate. Figure 3c presents that the free energy for H_2-to-methane is +5 kJ/mol H_2 at the threshold, a value similar to Fig. 2, since the final CH_4 concentrations are in the same range.

Figure 4 presents an experiment in which all methane was removed prior to the experiment, and a small amount of H_2 (55 nM) was added. The final methane concentration is 43 nM, and, as a result, the strict-thermodynamic threshold for methanogenesis is 0.2 nM. The biomass concentration initially is low (0.007 O.D.) and remains consistent throughout the experiment (Fig. 4b). Consumption of the low initial H_2 concentration and production of methane are simulated accurately by the model. The lower *b* (0.009/day) is in effect for the entire experiment, because the H_2 concentration is below the thermodynamic threshold when we strip H_2 and CH_4 at the start of the experiment; thus, the cells are in the survival state from the outset. H_2 oxidation stops at 0.7 nM, a value similar to our previous threshold, but higher than that (0.2 nM) depicted by thermodynamics of methanogenesis. In this case, the thermodynamics of the H_2-to-biomass control when H_2 oxidation stops in the model, and $\Delta G = 0$ stops this reaction.

The model highlights three phenomena that ought to affect competition among H_2-oxidizing microorganisms that perform different types of respiration: the kinetic threshold, the actual strict-thermodynamic threshold for H_2 oxidation, and the entry into survival mode.

The kinetic threshold, S_{min}, occurs naturally in the model when the H_2 concentration is ~2,400 nM for *M. bryantii* (Karadagli and Rittmann 2005). Our S_{min} value is comparable to the literature S_{min} value (~1,300 nM) reported for methanogens utilizing H_2 as the sole electron donor (Brown et al. 2005). For comparison of S_{min} values among different H_2 oxidizing groups, we selected a few representative microorganisms based on availability of all relevant kinetic parameters and computed S_{min} values (Table 2). S_{min} values in Table 2 indicate that methanogens are at disadvantage compared to sulfate reducers and dehalogenators when H_2 concentration is at the micromolar level.

Our experimental results are consistent with the model in that H_2 oxidation and methane formation are uncoupled in *M. bryantii* M.o.H., since methane production is irreversible. As discussed in detail by Karadagli and Rittmann (2006, companion), empirical H_2 thresholds for microorganisms using oxygen, nitrate, iron reduction, and sulfate seem to be similar to 0.4 nM, even though the strict thermodynamic thresholds for the terminal electron acceptor are much lower. This set of observations suggests that the H_2-to-solid-biomass threshold may take precedence, a hypothesis supported by the results in Fig. 4. If this is the case, then no group of respirers will have a strong competitive advantage when the H_2 concentration is low, around 1 nM.

The onset of the starvation-survival phase, represented by a tenfold decrease in the decay rate in the model, represents a strong competitive advantage for microorganisms that have this capability when the H_2 concentration is exceptionally low, less than 0.4 nM in the case of *M. bryantii.* The experimental results with *M. bryantii* support that this methanogen has such a strategy and may be espe-

Table 2 Computed S_{min} values for representative microorganisms with kinetic parameters obtained from literature

Microorganism	μ_{max} (1/day)	K_s (nM)	*b* (1/day)	S_{min} (nM)	Reference
Desulfovibrio vulgaris (Marburg)	3.6	1,300	0.09[a]	33	Kristjansson et al. (1982)
Methanospirillum hungatei JF-1	1.27	6,500	0.09	495	Robinson et al. (1984)
Methanobacterium bryantii M.o.H.	0.77	18,000	0.09	2,380	Karadagli and Rittmann (2005)
Dehalobacter restrictus	0.89	100[b]	0.09	11	Holliger et al. (1998)

[a] We used our endogenous decay constant for all microorganisms (Karadagli and Rittmann 2005), since this value is not provided in the relevant references

[b] A general K_s value for dehalogenators using H_2 (Smatlak et al. 1996)

cially good at surviving extended periods of H_2 depletion.

Conclusions

The new model captures the following aspects of H_2 oxidation and the H_2 threshold for *M. bryantii* M.o.H.:

- S_{min} occurs naturally for H_2 concentration near 2,400 nM, when the specific growth rate shifts from positive to negative.
- CH_4 generation from H_2 oxidation stops when $\Delta G = 0$ for the reaction of H_2 oxidation coupled to CH_4 generation. H_2 oxidation can continue beyond this point, making $\Delta G > 0$ for methanogenesis. Methanogenesis from oxidation of biomass continues.
- H_2 oxidation stops when $\Delta G = 0$ for transfer of electrons from H_2 to the solid-phase biomass component, which occurs $[H_2] = 0.4$ nM. This is the strict-thermodynamic threshold for H_2 oxidation.
- The shift to survival mode occurs after about 2 days from the time when $\Delta G = 0$ kJ/mol H_2 for the reaction between H_2 and solid-phase biomass component. Starvation survival is represented in the model by reducing the decay rate from 0.09 to 0.009/day 2 days after $\Delta G = 0$ kJ/mol H_2 for biomass as the electron acceptor.

The phenomena represented in the model have implications on the competitiveness of different microorganisms that oxidize H_2. When the H_2 concentration is high—well above the thermodynamic threshold—kinetics and S_{min} control, which microorganisms will prevail based on their ability to have a positive growth rate and consume H_2. As the H_2 concentration approaches the strict thermodynamic threshold of 0.4 nM, thermodynamics begin to dominate. If the H_2-to-solid-biomass threshold of ~0.4 nM is widespread among many types of H_2 oxidizers, no group of H_2 oxidizers should have a distinct thermodynamic advantage, even though the ΔG values for the terminal electron acceptors are widely different. Finally, the ability to initiate a starvation-survival strategy should give a long-term advantage to microorganisms exposed to very low H_2 concentrations.

References

Brown DG, Komlos J, Jaffé P (2005) Simultaneous utilization of acetate and hydrogen by Geobacter sulfurreducen and implications for use of hydrogen as an indicator of redox conditions. Environ Sci Technol 39:3069–3076

Chapelle FH, Haack SK, Adriaens P, Henry MA, Bradley PM (1996) Comparison of E_h and H_2 measurements for delineating redox processes in a contaminated aquifer. Environ Sci Technol 30:3565–3569

Conrad R (1996) Soil microorganisms as controllers of atmospheric trace gases (H_2, CO_2, CH_4, OCS, N_2O, and NO). Microbiol Rev 60:609–640

Cord-Ruwisch R, Seitz H-J, Conrad R (1988) The capacity of hydrogenotrophic anaerobic bacteria to compete for traces of hydrogen depends on the redox potential of the terminal electron acceptor. Arch Microbiol 149:350–357

Hoehler TM, Alperin MJ, Albert DB, Martens CS (1998) Thermodynamic control on hydrogen concentrations in anoxic sediments. Geochim Cosmochim Acta 62:1745–1756

Hollocher TC (1982) The pathway of nitrogen and reduction enzymes of denitrification. Antonie Leewenhoek J Microbiol 150:319–326

Holliger C, Han D, Harmsen H, Ludwig W et al (1998) *Dehalobacter restrictus* gen. nov. and sp. nov., a strictly anaerobic bacterium that reductively dechlorinates tetra- and trichloroethene in an anaerobic respiration. Arch Microbio 169:313–321

Karadagli F, Rittmann BE (2005) Kinetic characterization of *Methanobacterium bryantii* M.o.H. Environ Sci Technol 39:4900–4905

Karadagli F, Rittmann BE (2006, companion) Thermodynamic and kinetic analysis of the H_2 threshold for *methanobacterium bryantii* M.o.H. Biodegradation (in press)

Kjelleberg S, Hermansson M, Marden P, Jones GW (1987) The transient phase between growth and nongrowth of heterotrophic bacteria, with emphasis on the marine environment. Annu Rev Microbiol 41:25–49

Kristjansson JK, Schönheit P, Thauer RK (1982) Different K_s values for hydrogen of methanogenic bacteria and sulfate reducing bacteria. Arch Microbiol 131:278–282

Legall J, Fauque G (1988) Dissimilatory Reduction of sulfur compounds. In: Zehnder AJB (ed) Biology of anaerobic microorganisms. Wiley, New York, pp 469–585

Lovley DR (1985) Minimum threshold for hydrogen metabolism in methanogenic bacteria. Appl Environ Microbiol 49:1530–1531

Lovley DR, Goodwin ST (1988) Hydrogen concentrations as an indicator of the predominant terminal electron-accepting reactions in aquatic sediments. Geochim Cosmochim Acta 52:2993–3003

Namkung E, Rittmann BE (1987) Evaluation of bisubstrate secondary utilization kinetics by biofilms. Biotechnol Bioeng 29:335–342

Nicholls DG, Ferguson SJ (2002) Bioenergetics 3. Academic Press, London

Reeve AC, Bockman AT, Matin A (1984a) Role of protein degradation in the survival of carbon-starved *Escherichia coli* and *Salmonella typhimurium*. J Bacteriol 157:758–763

Reeve AC, Amy PS, Matin A (1984b) Role of protein synthesis in the survival of carbon-starved *Escherichia coli* K-12. J Bacteriol 160:1041–1046

Rittmann BE, McCarty PL (2001) Environmental biotechnology: principles and applications. McGraw-Hill, New York

Robinson JA, Tiedje JM (1984) Competition between sulfate-reducing and methanogenic bacteria for H_2 under resting and growing conditions. Arch Microbiol 137:26–32

Smatlak CR, Gossett JR, Zinder SH (1996) Comparative kinetics of hydrogen utilization for reductive dechlorination of tetrachloroethene and methanogenesis in an anaerobic enrichment culture. Environ Sci Technol 30:2850–2858

Stumm W, Morgan JJ (1996) Aquatic Chemistry: Chemical equilibria and rates in natural waters, 3rd edn. Wiley, New York

Stouthamer AH (1988) Dissimilatory reduction of oxidized nitrogen compounds. In: Zehnder AJB (ed) Biology of anaerobic microorganisms. Wiley, New York, pp 179–244

Siegele DA, Kolter R (1992) Life after Log. J Bacteriol 174:345–348

Thauer RK (1998) Biochemistry of methanogenesis: a tribute to Marjory Stephenson. Microbiology 144:2377–2406

Valentine DL, Blanton DC, Reeburgh WS (2000) Hydrogen production by methanogens under low-hydrogen conditions. Arch Microbiol 174:415–421

Widdel F (1988) Microbiology and ecology of sulfate- and sulfur-reducing bacteria. In: Zehnder AJB (ed) Biology of anaerobic organisms. Wiley, New York, pp 469–585

Yang Y, McCarty PL (1998) Competition for hydrogen within a chlorinated solvent dehalogenating anaerobic mixed culture. Environ Sci Technol 32:3591–3597